FINAL TECHNICAL REPORT

Determining slip per event on the San Andreas fault from fold deformation at the Frazier Mountain site

Recipient:

[1]University of Oregon
Department of Geological Sciences
1272 University of Oregon Eugene, OR 97403-1272
tel (541) 346-4584; fax (541) 346-4692; URL http://pages.uoregon.edu/dogsci/doku.php

Principal Investigators:

Ray J. Weldon II [1], Ashley R. Streig [2], David Schmidt[3]
ray@uoregon.edu[1], streig@uoregon.edu[2], dasc@uw.edu[3]

Collaborators:
Katherine Scharer, Tom Fumal
U.S. Geological Survey

Keywords:

Southern San Andreas fault, slip per event, transtensive step-over, fold deformation

Program Element III

U. S. Geological Survey
National Earthquake Hazards Reduction Program
Award Number G11AP201223

September 2013

Research supported by the U.S. Geological Survey (USGS), Department of the Interior, under USGS award number G11AP20123. The views and conclusions contained in this document are those of the authors and should not be interpreted as necessarily representing the official policies, either expressed or implied, of the U.S. Government.

Award G11AP201223

Determining slip per event on the San Andreas fault from fold deformation at the Frazier Mountain site

Ray J. Weldon II [1], Ashley R. Streig [2] and David Schmidt[3]
ray@uoregon.edu[1], streig@uoregon.ed[2], dasc@uw.edu[3]

ABSTRACT

Transtensive step-overs known as sags are among the most ubiquitous features of strike slip faults. These structures create closed depressions that collect sediment, are often wet, and thus preserve organic material that can be used to date the thick and rapidly accumulating section. It is clear from historical ruptures that these depressions grow incrementally with each earthquake. We are developing methods to carefully document and separate individual folding events, and to relate the amount of sagging or folding to the amount of horizontal slip creating the sag, with the goal of generating slip per event chronologies. This will be useful as sags are often the best sites for preserving evidence of earthquake timing, and determining slip at these sites will eliminate the ambiguity inherent in tying earthquake age data from micro-stratigraphic sites to nearby undated sites with good micro-geomorphic slip evidence. We apply this approach to the Frazier Mountain site on the Southern San Andreas fault where we integrate trenching, cone penetrometer testing (CPT), surveying, photomosaicing, B4 LiDAR data and GIS techniques to make a detailed 3D map of subsurface geology, fault traces and related folds across the site. These data are used to generate structure contour and isopach maps for key stratigraphic units in order to evaluate fold deformation of paleo-ground surfaces across a transtensional step-over on the San Andreas fault.

Award G11AP201223

Determining slip per event on the San Andreas fault from fold deformation at the Frazier Mountain site

Ray J. Weldon II [1], Ashley R. Streig [2] and David Schmidt[3]
ray@uoregon.edu[1], streig@uoregon.ed[2], dasc@uw.edu[3]

ABSTRACT

Transtensive step-overs known as sags are among the most ubiquitous features of strike slip faults. These structures create closed depressions that collect sediment, are often wet, and thus preserve organic material that can be used to date the thick and rapidly accumulating section. It is clear from historical ruptures that these depressions grow incrementally with each earthquake. We are developing methods to carefully document and separate individual folding events, and to relate the amount of sagging or folding to the amount of horizontal slip creating the sag, with the goal of generating slip per event chronologies. This will be useful as sags are often the best sites for preserving evidence of earthquake timing, and determining slip at these sites will eliminate the ambiguity inherent in tying earthquake age data from micro-stratigraphic sites to nearby undated sites with good micro-geomorphic slip evidence. We apply this approach to the Frazier Mountain site on the Southern San Andreas fault where we integrate trenching, cone penetrometer testing (CPT), surveying, photomosaicing, B4 LiDAR data and GIS techniques to make a detailed 3D map of subsurface geology, fault traces and related folds across the site. These data are used to generate structure contour and isopach maps for key stratigraphic units in order to evaluate fold deformation of paleo-ground surfaces across a transtensional step-over on the San Andreas fault.

TABLE OF CONTENTS

Abstract i
1.0 Introduction 1
2.0 Frazier Mountain Site 3
2.1 Paleoseismic Results 3
2.2 Explanation & Methods: 2-D Retrodeformation of fold horizons 5
3.0 Significance of Study 10
4.0 Acknowledgements 11
5.0 References 12

LIST OF FIGURES

Figure 1. Frazier Mountain site map 2
Figure 2. Photographs showing folding of unit 5 3
Figure 3. Oblique & 3D view of the distribution of trenches and data across the northwestern sag at the Frazier mountain site 4
Figure 4. Photomosaic trench logs for Trench 1 cut 1 west and Trench 1 cut 3 6
Figure 5. T23 - Photomosaic trench log & 2D reconstruction 7
Figure 6. T28 - Photomosaic trench log & 2D reconstruction 8
Figure 7. T30 - Photomosaic trench log & 2D reconstruction 9
Figure 8. Preliminary structural contour map for the northwestern syncline. 10

1.0 INTRODUCTION

The Frazier Mountain paleoseismic site is located at the northwest end of the Mojave section of the San Andreas Fault, near the junction with the Garlock fault (34.8122°, -118.8122°, 1279 m; Figure 1). The site is located along a releasing step on the Southern San Andreas fault in the transpressive 'big bend region' north of Los Angeles. Frazier trenches clearly show the main active trace of the San Andreas fault right stepping ~30 m over ~100 m along strike, producing two synclines that dramatically thicken the stratigraphic section. Earthquakes rupturing through the site have repeatedly produced a small depression or sag on the surface which is subsequently infilled with sand and silt deposits. 34 paleoseismic trenches show stratigraphic and structural relationships spanning the sag, and demonstrate progressive fold deformation across two depocenters separated by a low relief intra-basin high. Earthquake evidence includes offset stratigraphy across graben bounding faults, upward fault terminations, fissures, progressive sag (fold) deformation of stratigraphy and growth strata sequences above earthquake horizons.

Relationships observed in trenches reveal that the western syncline is both wider and deeper than the eastern syncline. The western syncline is roughly 60 meters long, 30 meters wide and records 5 earthquakes within a 5 meter thick section, whereas the eastern syncline is shorter, narrower and shallower. The eastern sag is 15 to 20 meters long, 10 meters wide, and here evidence for earthquake 5 is about 2.5 meters below the ground surface. Trench exposures across both sags show that the syncline axis slightly changes orientation from event to event, complicating simple interpretations of growth strata and fold evidence for multiple earthquakes. We generated a database of folded stratigraphic units from trench data to investigate and compare the 2D and 3D shape and extent of fold and fault deformation between unit horizons. We use these data to generate preliminary isopach maps highlighting complex relationships between fold geometry and growth strata for several earthquake event horizons. We use these data to compare the areal extent of folding associated with each horizon in the northwestern sag and the amount of fold relief generated by each of the last 5 earthquakes.

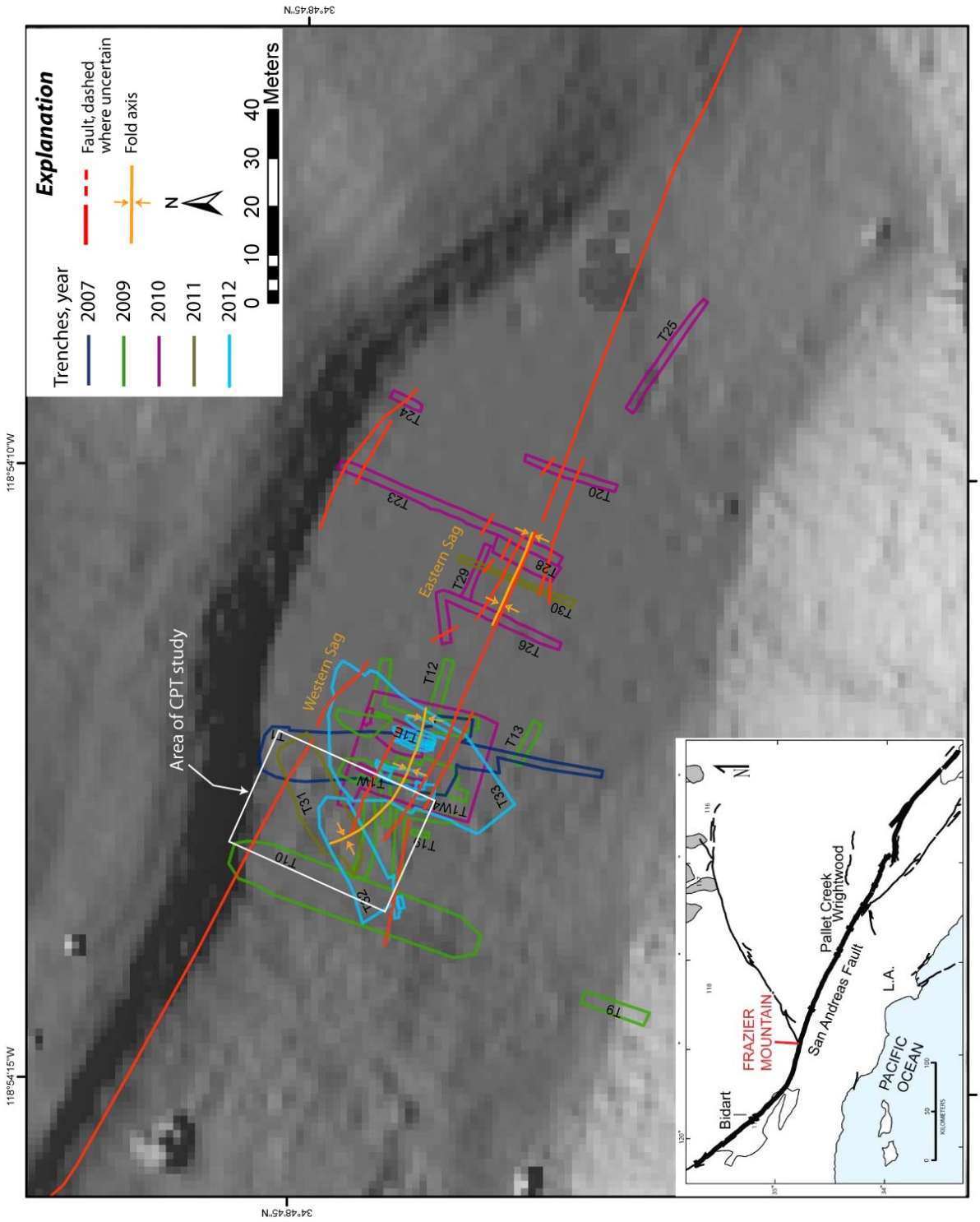

Figure 1. Frazier Mountain site map showing locations of trenches excavated in 2008, 2009, 2010, 2011 and 2012. Fault and syncline axis locations are constrained by trench exposures of the structures and are shown as red and orange lines on the map, respectively. Inset shows the location of the Frazier Mountain site on the Southern San Andreas fault, southern California. Basemap: shaded relief compiled from GeoEarthScope B4 LiDAR data (DOI: 10.5069/G97P8W9T).

2.0 FRAZIER MOUNTAIN SITE

2.1 Paleoseismic Results

Approximately 34 trenches show the main active trace of the San Andreas fault right stepping ~30 m over ~100 m along strike producing two small synclinal sags that dramatically thicken the stratigraphic section (Figure 1). The Frazier Mountain site has yielded good earthquake chronologies, and relationships between fold deformation and surface fault rupture for the last 5 earthquakes. We observe that the degree of sagging in the synclines varies along strike for each feature, but that the ratio of fold deformation between earthquake horizons remains constant in both synclines. The penultimate earthquake, E2, produced a depression that was infilled by unit 5, a gravel (Figure 2), which was subsequently folded in the most recent earthquake in 1857 (Figure 3). Fine-grained alluvial units overlie the gravel and fill the 1857 depression such that the current surface is relatively horizontal.

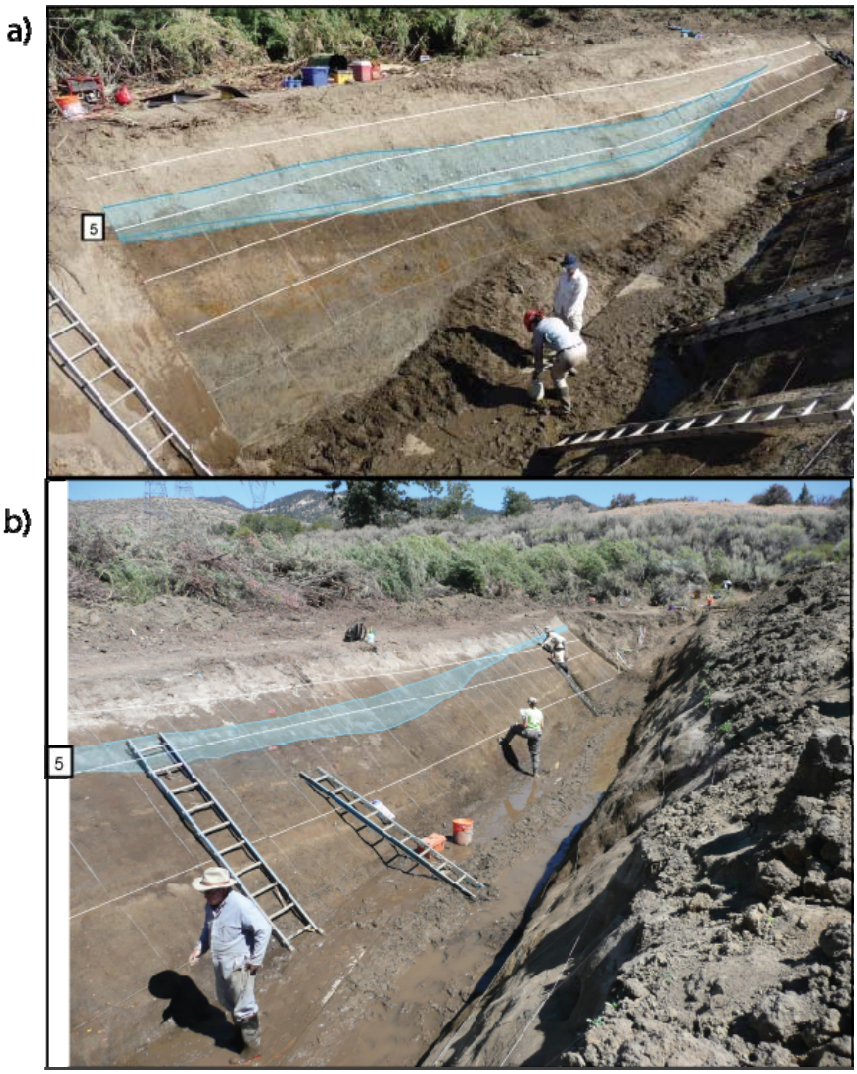

Figure 2. Photographs showing folding of unit 5, 'blue gravel unit', shown as a blue polygon in both photos. a) Photo of trench T10E and b) Trench T1W cut1. The base of unit 5 drops about ~1 meter from the outer edges of the fold limbs to the fold axis. Unit 5 thickens in the fold axis, and is twice as thick in center of fold as the limbs of the fold. Unit 5 gravel deposit, also thickens to the northwest, nearest the sediment source, to southeast. The northwest thickening of unit 5 is shown here; T10 is the western most trench and is closer to the source than all other trenches. The blue gravel is thicker in a) T10 than in photo b) T1. [Note: The apparent warping of the white grid in the upper photos (T10E) is due to an irregular wall and the perspective of the photo; the grid is really horizontal and spaced 50 cm apart vertically.]

We have continuous 3-D data for three earthquake horizons, E2, E3 and E5, in the western sag, shown by the blue, purple and yellow points in Figure 3. Unit 35, shown as the yellow horizon throughout this report, was deposited soon after E5, the fifth event back. Unit 18, shown as the purple horizon in this report, was the ground surface during E3, the third youngest event. Unit 5, shown as blue is present in the in the larger, western sag. Unit 5 fills a depression formed by the penultimate earthquake, and is deformed by the most recent earthquake, 1857. However, a fine-grained facies of this unit is only recognized in trench T23, in the eastern sag. We provide photomosaic trench logs and 2-D retrodeformation of these event horizons in section 2.2.

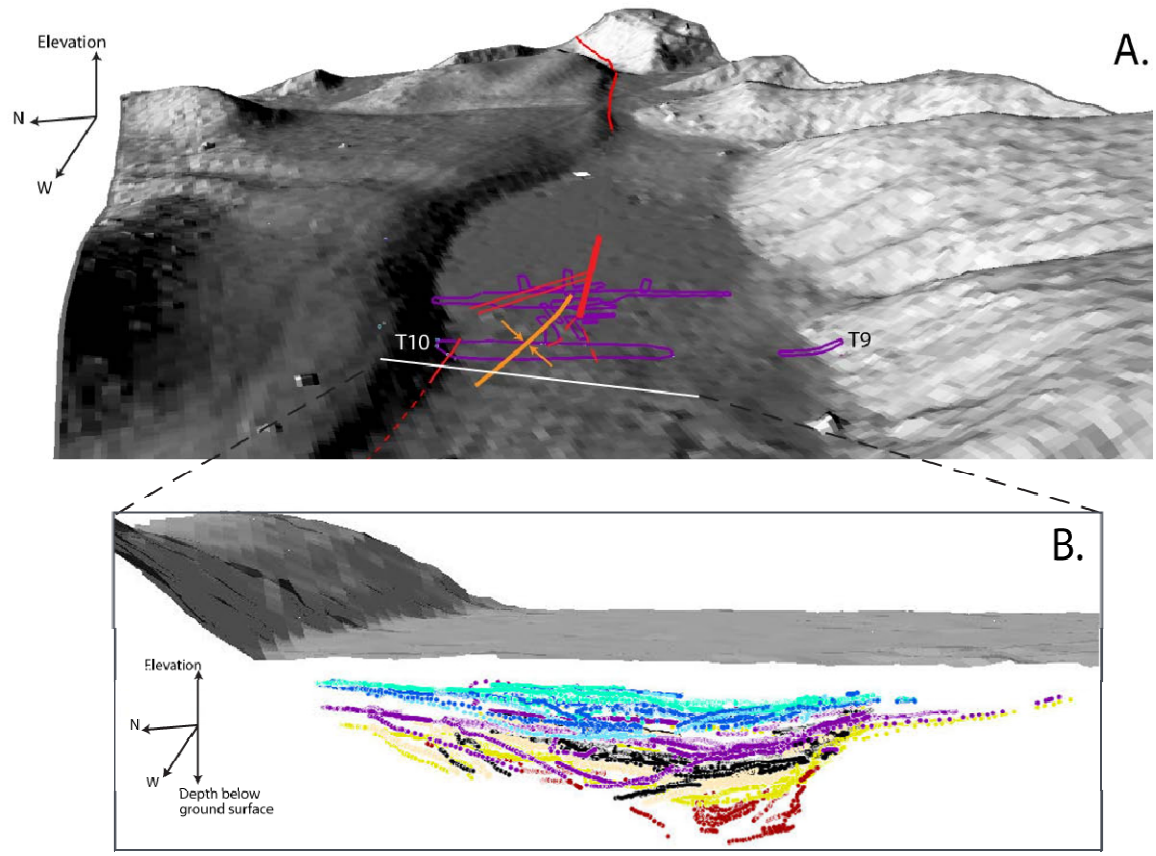

Figure 3. Oblique view of the distribution of trenches across the northwestern sag at the Frazier mountain site. A.) Hillshade derived from B4 lidar data with paleoseismic trench locations, fault traces and fold axis across the northwestern sag (For complete map of trenches and structures see Figure 1). B.) 3-D cross sectional view showing folded stratigraphic horizons across the northwestern sag, looking toward the southeast roughly along the northwestern wall of T10. Colored points below the ground surface are stratigraphic unit horizons logged and surveyed during paleoseismic excavations (stratigraphy exposed in 2007, 2009, 2010, 2011 and 2012). Unit horizons are correlated between trenches and are color coded by unit, with 5x vertical exaggeration of topography shown in A. Blue points are the base of unit 5 which fills a depression formed by the penultimate and is folded by 1857, and unit 6 is folded by two earthquakes. Yellow points are the base of unit 18, and have been folded by three earthquakes. Yellow points are the base of unit 35, and have been deformed by 5 earthquakes. Unit 53 is the deepest unit shown here as dark red points, shows the greatest degree of folding, and has been folded and faulted by 7 earthquakes.

2.2 Explanation & Methods: 2-D Retrodeformation of fold horizons

We correlate stratigraphic units between the large western sag and the smaller eastern sag, and provide simplified photomosaic trench logs with key stratigraphic unit horizons highlighted by unit in this report (Figures 4 – 7). Photomosaic trench logs for Trench 1 cut 1 west and Trench 1 cut 3 west show broader fold deformation across the larger, wider, western sag (Figure 4). Photomosaic trench logs for the east wall of trench 23 (Figure 5, inverted photomosaic), the west wall of trench 28 (Figure 6), and the west wall of trench 30 (Figure 7) show fold deformation across the smaller eastern sag (see Figure 1). Earthquake horizons E2, E3 and E5 are shown by bold lines on trench logs and correspond with unit horizons 5 (blue), 18 (purple) and 35 (yellow), respectively. Faults are shown as red lines.

The base of the 'blue gravel unit' unit 5, reflects folding from 1857 and the penultimate E2 earthquake. Unit 18 (purple) a fine grained sand and silt sequence that has been deformed by 3 earthquakes, and unit 35 (yellow) which has been deformed by 5 earthquakes. We remove fold deformation for each of these horizons in successive iterations, from younger (E2 horizon) to the earthquake E5 horizon. We did this by exporting coordinates from our ArcGIS database for the depth of each folded unit (5, 18 and 35) below the ground surface with distance along the trench wall (e.g. Figures 4 – 7).

As shown in Figure 3, the stratigraphic section thickens across each fold. We "tilt" each contact to remove the linear thickening from the section. This can be seen in Figures 4, 5 and 6, where unit 18 (purple) and unit 35 (yellow) align on the south (left) side but not on the north (right). We then subtract unit 18 (purple) from unit 35 (yellow). This is shown as 'yellow minus purple' in Figures 4 – 7, and shows in 2D what the fold geometry of the yellow surface would have been after E5, and before subsequent earthquakes occurred. We also subtract unit 5 (blue) from unit 18 (purple) if unit 5 is present (and recognized). While this is not a physically perfect way to unfold, these folds are so broad and shallow (2-D retrodeformation figures have 2-10 times vertically exaggeration) that this simple approach gives us illustrative results. In some cases we also remove subsequent fault slip (shown in red ellipses in Figure 6); fault slip is largely lateral and juxtaposes different thicknesses of section, so removing it in this way effectively aligns sections of the same thickness (Figure 6).

E2 (unit 5, blue points) has double the observed folding associated with the 1857 event in the core of the NW syncline (Figure 4). Based on these trench exposures, it appears that the past 3 events were about the same size as the previous 2. In all of these examples E5, unit 35, is about twice as folded as E3, unit 18 (shown on 2D retrodeformation by yellow-unit 35 minus purple-unit 18, Figures 4-7). We find that earthquake E5 (unit 35) has nearly double the amount of fold deformation observed across the E3 (unit 18) paleo-surface in both sags, and three times the deformation observed on the E2 (unit 5) surface in the NW sag. Ratios of fold deformation between events are E2 = 2*E1, E5 = 3*E2, and E5 = 2*E3.

a)

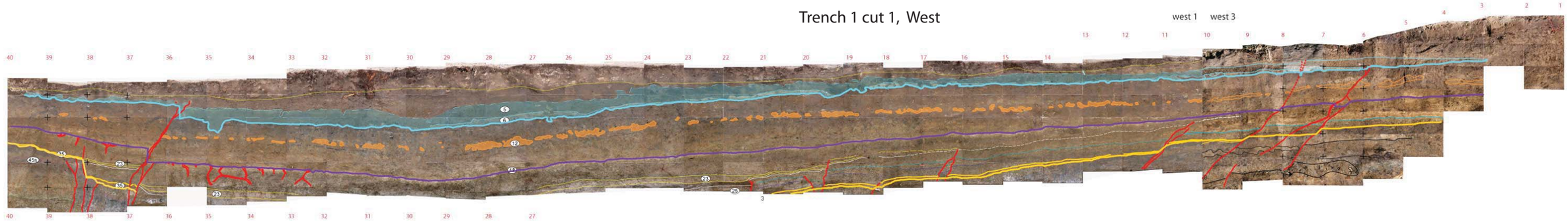

b)

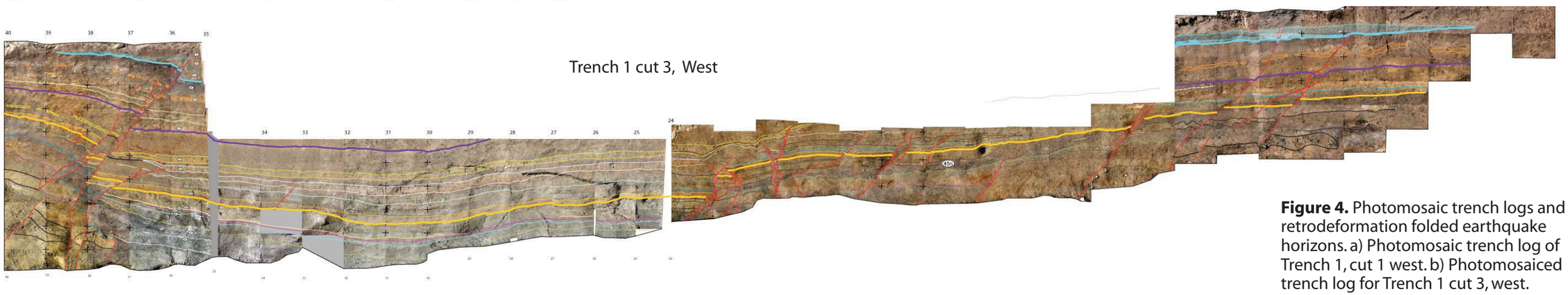

c)

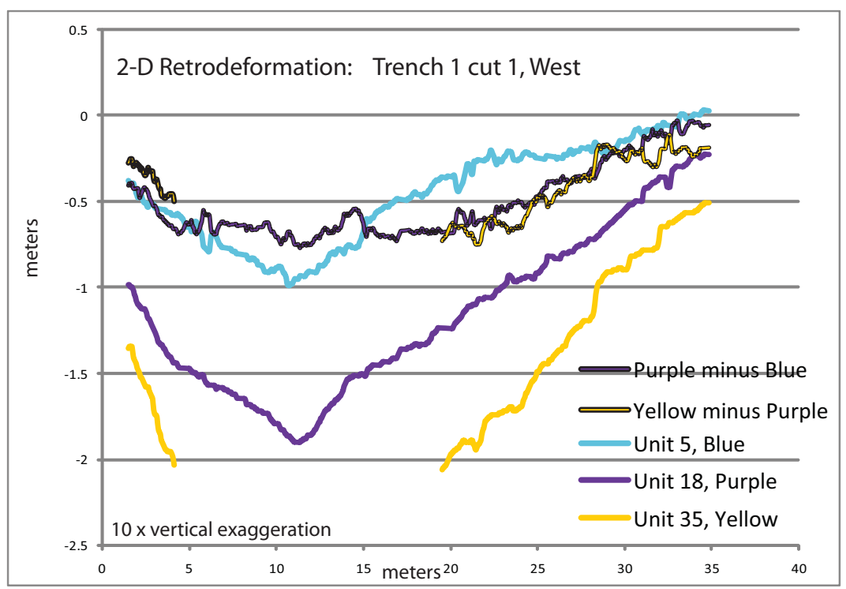

d)

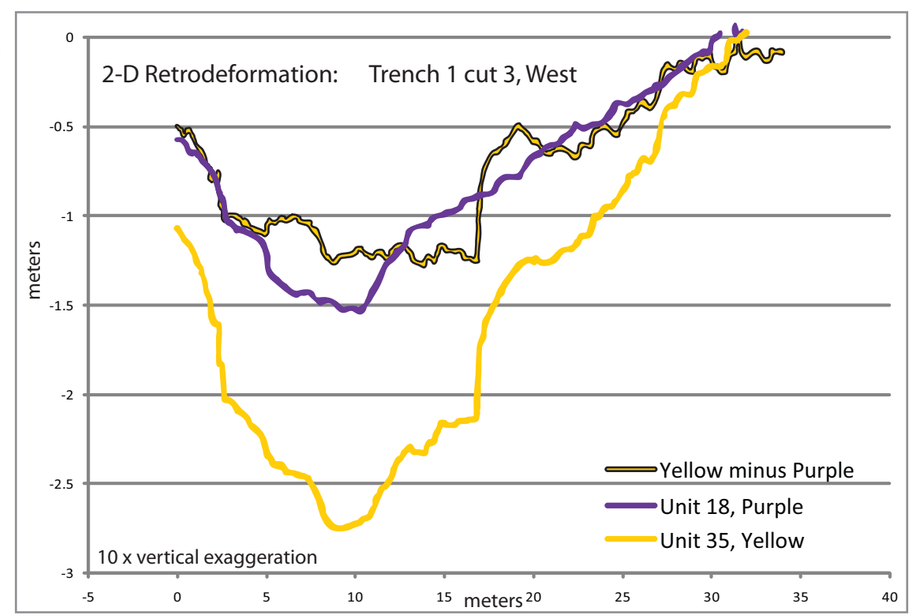

Figure 4. Photomosaic trench logs and 2-D retrodeformation folded earthquake horizons. a) Photomosaic trench log of Trench 1, cut 1 west. b) Photomosaiced trench log for Trench 1 cut 3, west. Earthquake horizons are shown by bold lines, corresponding with unit 5 (blue), unit 18 (purple) and unit 35 (yellow). Faults are shown as red lines. Folding of the double yellow unit is two times as great as the overlying purple unit. We interpret 3 events to have occurred since deposition of purple, and 6 events to have occurred since deposition of double yellow. c) 2-D retrodeformation of blue, purple and yellow horizons in Trench 1, cut 1. In the upper (cut 1) it appears that purple is deformed about twice as much as blue. Because purple is 3 events and blue 2, it suggests that the purple event was about as large at the most recent 2 events together. d) 2-D retrodeformation of purple and yellow horizons in trench 1 cut 3. In the lower (cut 3) it appears that double yellow is deformed about twice as much as blue. Because purple is 3 events and double yellow lies between events 5 and 6 , it appears that the last 3 events were about as large at the previous 3 events.

a) Trench 23 East (inverted)

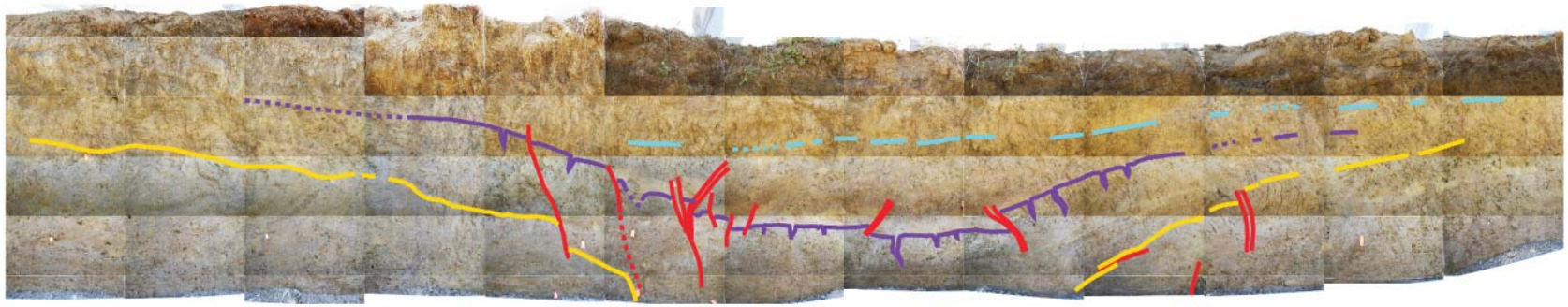

b)

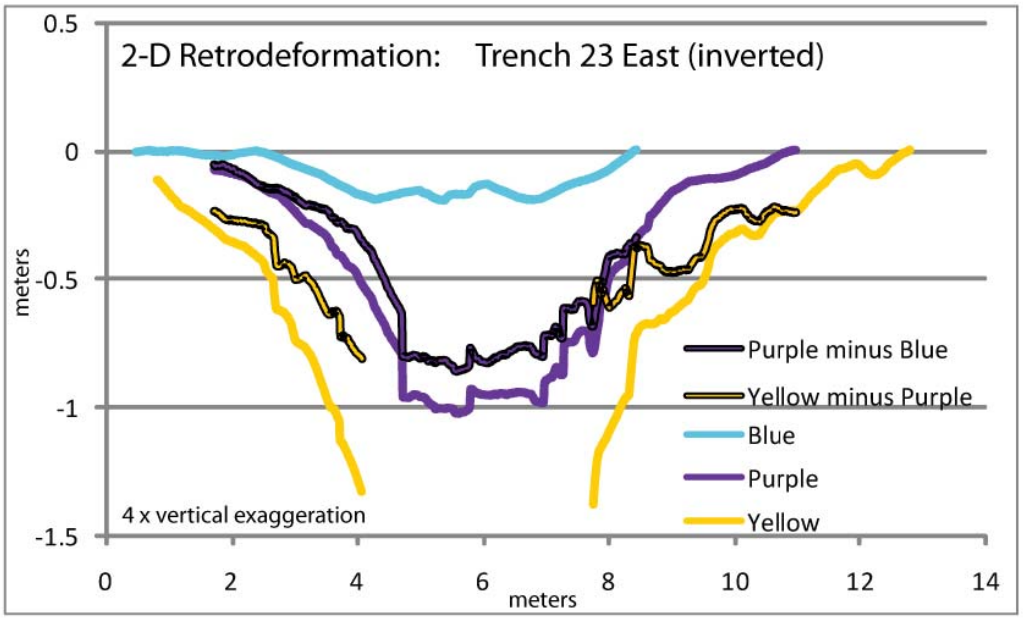

Figure 5. Photomosaic trench logs and 2-D retrodeformation folded earthquake horizons. a) Photomosaic trench log of Trench 23 East. Earthquake horizons are shown by bold lines, corresponding with unit 5 (blue), unit 18 (purple) and unit 35 (yellow). Faults are shown as red lines. b) 2-D retrodeformation of blue, purple and yellow horizons in Trench 23. Unit 35, yellow, is twice as folded as unit 18, purple, as shown by the black outlined yellow line representing the yellow surface minus fold geometry for the purple surface.

a) Trench 28 West

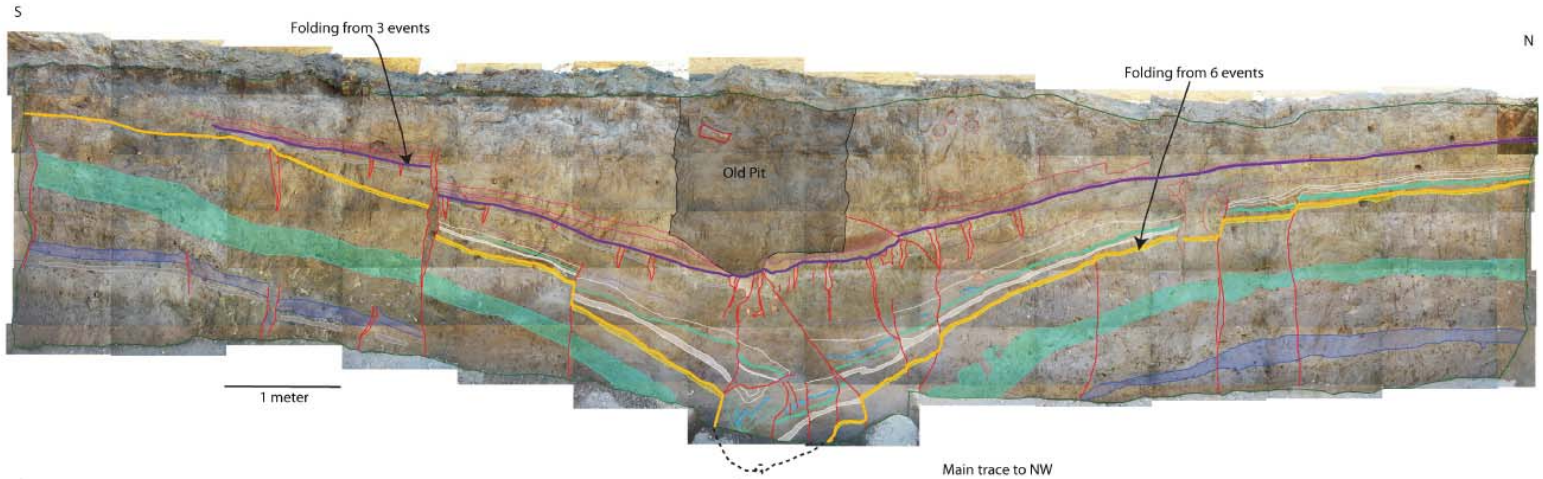

b)

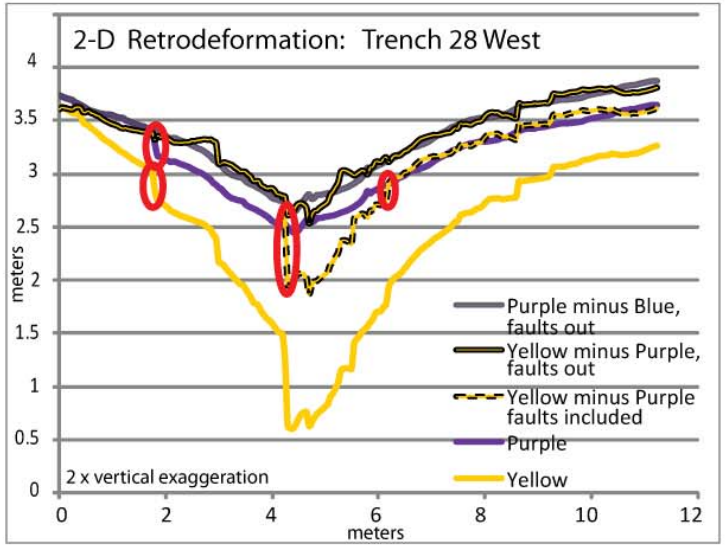

Figure 6. Photomosaic trench logs and 2-D retrodeformation folded earthquake horizons. a) Photomosaic trench log of Trench 23 East. Earthquake horizons are shown by bold lines, corresponding with unit 18 (purple) and unit 35 (yellow). Faults are shown as red lines. b) 2-D retrodeformation of purple and yellow horizons in Trench 28. Unit 35, yellow, is twice as folded as unit 18, purple, and is shown by the black outlined yellow line which represents the yellow surface minus fold geometry for the purple surface, and lateral slip along faults has been removed. The red ellipses show fault locations. Fault slip is largely lateral and juxtaposes different thicknesses of section, so we remove fault slip by removing this vertical separation, this effectively aligns sections of the same thickness.

a) Trench 30 West

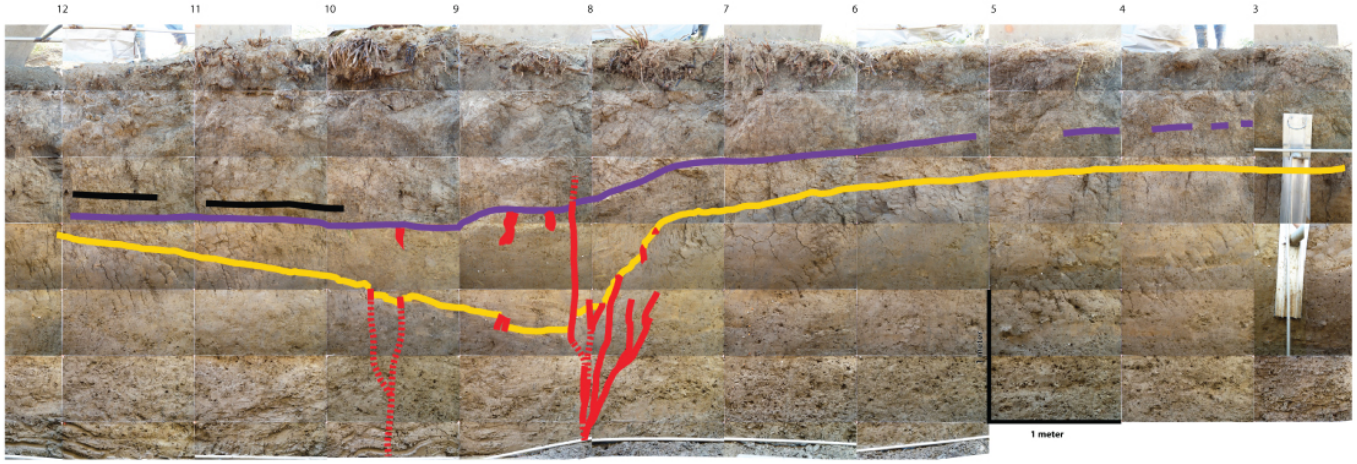

b)

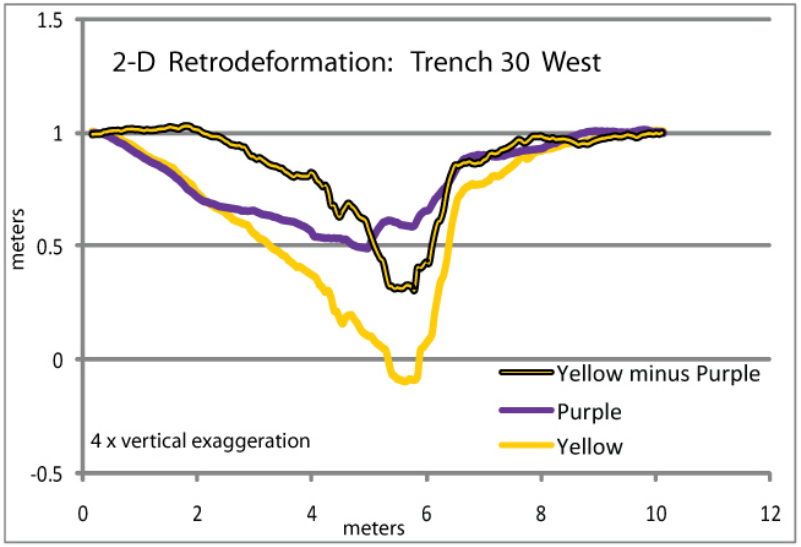

Figure 7. Photomosaic trench logs and 2-D retrodeformation folded earthquake horizons. a) Photomosaic trench log of Trench 30 West. Earthquake horizons are shown by bold lines, corresponding with unit 5 (blue), unit 18 (purple) and unit 35 (yellow). Faults are shown as red lines. b) 2-D retrodeformation of blue, purple and yellow horizons in Trench 30. Unit 35, yellow, is twice as folded as unit 18, purple, as shown by the black outlined yellow line that represents the yellow surface minus fold geometry for the purple surface.

Lastly, we have generated a preliminary structure contour map for the larger, northwestern sag using stratigraphic unit elevation data from T1-4W, T11, T14, T15, T18, and T19 (Figure 8). Unit 5, blue gravel filled the folded surface created by the penultimate event and is also folded by the 1857 earthquake, so the ~ 130 cm of relief is caused by two events (Figure 8).

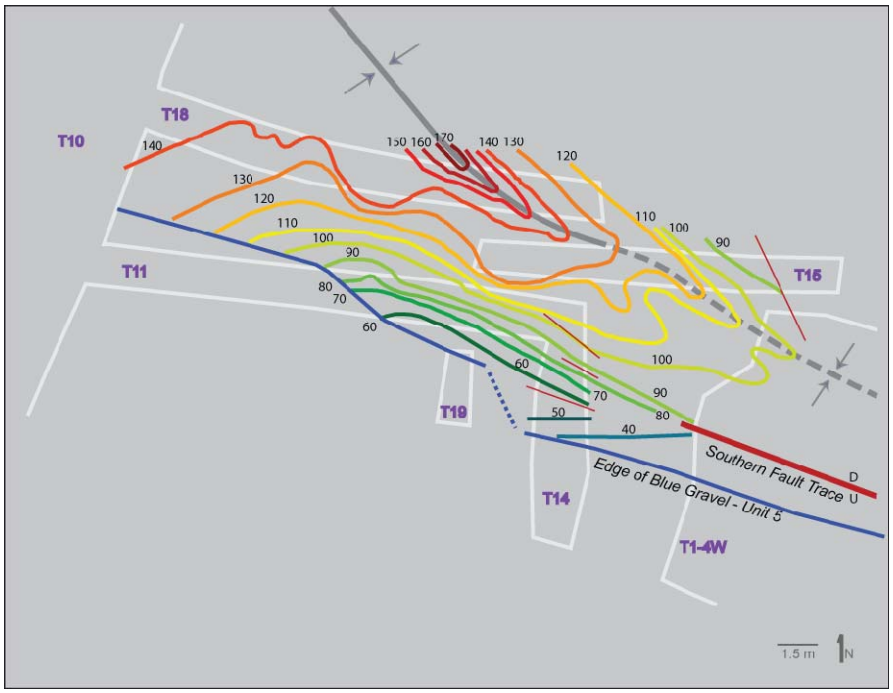

Figure 8. Preliminary structural contour map for the northwestern syncline. Multi-colored contours show the depth to the base of unit 5 "blue gravel". White lines show the trench locations, dark blue lines mark the edge of the blue gravel. Unit 5, the blue gravel pinches out to the south against relief that was generated by the intersection of the fold and the fault tip. At this intersection, older units preserve the folding and younger units overlap this edge. Unit 5, blue gravel, filled the folded surface created by the penultimate event and is also folded by the 1857 earthquake, so the ~ 130cm of relief is caused by two events. Note how the syncline widens and deepens to the northwest.

3.0 SIGNIFICANCE OF STUDY

We can quantify folding in individual ruptures across this step-over using three dimensional point data for stratigraphic surfaces. The most significant finding of this preliminary structural analysis is that the surface of the step-over dropped by transtensional faulting and warping approximately 50 to 100 cm during each of the last 5 earthquakes. Due to the large number of trenches, we have not yet completely quantified analysis of slip per event. However, using generic vertical to horizontal slip ratios from transtensional basins across the globe (1:4), we can infer that each earthquake produced at least ~2 m of horizontal slip at the site. Structural modeling of the main fault zone shows a maximum slip of 26 m was accommodated on this fault zone during the last 5 earthquakes. Trishear modeling of older events (earthquakes 6, 7, and 8) suggests that ~3

m of vertical slip is required to produce the deformation expressed by these three events, supporting the inference that each of the earthquakes at Frazier produced 1-4 m of horizontal slip.

The most significant paleoseismic finding at the Frazier Mountain site is that since ca. 1400 AD, the earthquake history at Frazier Mountain is fairly similar to the published record from the Bidart Fan site (Akciz et al., 2010), but quite different from the neighboring Pallett Creek site (Scharer et al., 2011; Scharer et al., *paper in prep.*). It appears, for example, that in the 450 years prior to the historic 1857 earthquake, only one earthquake of comparable rupture length and magnitude occurred. Yet we found that the recurrence interval was quite short, on the order of 80 years during this period (Scharer et al., 2013). This requires that the Carrizo and Big Bend have smaller (perhaps M7.1) earthquakes that do not extend all the way into the Mojave section of the southern San Andreas Fault. These results contradict previous models for this part of the fault, which argued based on scant data that larger (M7.8) earthquakes occurred approximately every 250 years.

4.0 ACKNOWLEDGEMENTS

This work was funded by internal and external funds of the Earthquake Hazard Reduction Program of the U.S. Geological Survey and grants from the Southern California Earthquake Center and the National Science Foundation to the University of Oregon and Appalachian State University.

The fieldwork could not have been completed without the assistance of number of students and colleagues, including: Sequoia Alba, Hehewutei Amakali, Adam Arce, Lauren Austin, Sean Bemis, Reed Burgette, Tim Dawson, Teri Gerard, Brian Gibson, Chesney Gilleland, C Hilden, S Hunt, Andy Jerrett, Rachel Lippoldt, Cynthia Liutkus, Kate McGinnis, Jessica Norman, Aaron Pruitt, Carlos Reyes, Helen Mary Sheridan, Carl Swanson, LiLi Weldon, Nick Weldon, Nyle Weldon, Robert Sickler, Judy Zachariesen.

The hillshade in Figure 1 is derived from B4 LiDAR data, based on [data, processing] services provided by the OpenTopography Facility with support from the National Science Foundation under NSF Award Numbers 0930731 & 0930643. The B4 LiDAR Project collected LiDAR point cloud data of the southern San Andreas and San Jacinto Faults in southern California. Data acquisition and processing were performed by the National Center for Airborne Laser Mapping (NCALM) in partnership with the USGS and Ohio State University through funding from the EAR Geophysics program at the National Science Foundation (NSF). Optech International contributed the ALTM3100 laser scanner system. UNAVCO and SCIGN assisted in GPS ground control and continuous high rate GPS data acquisition. A group of volunteers from USGS, UCSD, UCLA, Caltech and private industry, as well as gracious landowners along the fault zones, also made the project possible. http://dx.doi.org/10.5069/G97P8W9T

5.0 REFERENCES

Akciz, S.O., Grant Ludwig, L., Arrowsmith, J R., Zielke, O., 2010. Century-long average time intervals between earthquake ruptures of the San Andreas fault in the Carrizo Plain, California :Geology, v. 38, p. 787 - 790.

Bronk Ramsey, C., 2009, OxCal Program, v.4.1.3, Radiocarbon Accelerator Unit, University of Oxford, Oxford, United Kingdom, https://c14.arch.ox.ac.uk/oxcal.html (last accessed on December 2011).

Crowell, J.C., 2003, Tectonics of Ridge Basin region, southern California, in Crowell, J.C., ed., Evolutionof Ridge Basin, Southern California: An Interplay of Sedimentation and Tectonics, GSA Special Paper367, p. 157-204.

Lindvall, S.C., Rockwell, T., Dawson, T., Helms, J., and Bowman, K.W., 2002, Evidence for Two SurfaceRuptures in the Past 500 Years on the San Andreas Fault at Frazier Mountain, California: Bulletin ofthe Seismological Society of America, v. 92, p. 2689-2703.

Scharer., K., Fumal, T., Weldon, R., Streig, A., *in press 2013*, Photomosaics and event evidence from the Frazier Mountain paleoseismic site, Trench 1 cuts 1-4 (2007-2009), U.S. Department of the Interior, U.S. Geological Survey, Open-File Report XXXX-XXXX

Scharer, K., Weldon, R., Gibson, B., and Streig, A., 2011, Earthquake ages and Displacements, Frazier Mountain Paleoseismic Site, American Geophysical Union, Fall Meeting 2011, Abstract #T51B-2324

Scharer, K.M., Weldon, R.J., Fumal, T.E., and Biasi, G.P., 2007, Paleoearthquakes on the southern SanAndreas fault, Wrightwood, CA 3000 to 1500 B.C.: a new method for evaluating paleoseismicevidence and earthquake horizons: Bulletin of the Seismological Society of America, v. 97, p. 1054-1093.

Working Group on California Earthquake Probabilities, 1988, Probabilities of large earthquakes occurring in California on the San Andreas fault, U.S. Geological Survey Open-File Report, p. 62.

Working Group on California Earthquake Probabilities, 1990, Probabilities of large earthquakes in the San Francisco Bay Region, California: U.S. Geological Survey Circular, p. 51.

Working Group on California Earthquake Probabilities, 2003, Earthquake Probabilities in the San Francisco Bay Region: 2002–2031: U.S. Geological Survey Open-File Report 03-214.

Working Group on California Earthquake Probabilities, 2008, The Uniform California Earthquake Rupture Forecast, Version 2 (UCERF 2): U.S. Geological Survey Open-File Report 2007-1437, 95 p.

Working Group on Northern California Earthquake Potential, 1996, Database of potential sources for earthquakes larger than magnitude 6 in northern California: U.S. Geological Survey Open-File Report 96-705, p. 53 p. [http://quake.wr.usgs.gov:80/hazprep/NCEP/].